Controlled Dispersion of the Extensional Wave in Composite Isotropic and Transversely Isotropic Rods
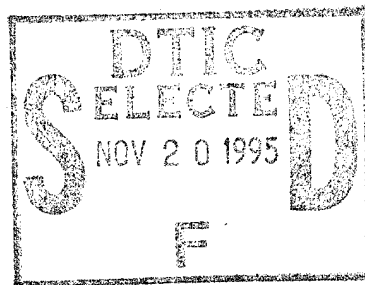
Marilyn J. Berliner
Submarine Sonar Department

DTIC
SELECTED
NOV 2 0 1995
F

19951116 093

Naval Undersea Warfare Center Division
Newport, Rhode Island

DTIC QUALITY INSPECTED 3

PREFACE

This document was prepared under Project No. B10003, *Stress Wave Propagation in a Layered Elastic and Viscoelastic Transversely Isotropic Cylinder Immersed in an Acoustic Medium*. It was sponsored by the NUWC Independent Research (IR) Program, program manager Dr. S. C. Dickinson. The IR program is funded by the Office of Naval Research.

The technical reviewer for this report was Dr. Bruce E. Sandman (Code 823).

REPORT DOCUMENTATION PAGE

1. AGENCY USE ONLY (Leave Blank)	2. REPORT DATE 14 August 1995	3. REPORT TYPE AND DATES COVERED Final

4. TITLE AND SUBTITLE

Controlled Dispersion of the Extensional Wave in Composite Isotropic and Transversely Isotropic Rods

5. FUNDING NUMBERS

6. AUTHOR(S)

Marilyn J. Berliner

7. PERFORMING ORGANIZATION NAME(S) AND ADDRESS(ES)

Naval Undersea Warfare Center
Detachment New London
New London, Connecticut 06320

8. PERFORMING ORGANIZATION REPORT NUMBER

TR 11,029

9. SPONSORING/MONITORING AGENCY NAME(S) AND ADDRESS(ES)

10. SPONSORING/MONITORING AGENCY REPORT NUMBER

11. SUPPLEMENTARY NOTES

12a. DISTRIBUTION/AVAILABILITY STATEMENT

Approved for public release; distribution is unlimited.

12b. DISTRIBUTION CODE

13. ABSTRACT (Maximum 200 words)

The dispersion of extensional waves in composite isotropic and transversely isotropic rods is investigated. The equations of motion of an infinitely long, layered rod with a transversely isotropic core and transversely isotropic casing are developed using the three-dimensional equations of elasticity. Simplifications to the equations of motion for axisymmetric modes of wave propagation and for material isotropy are presented. Methodologies for controlling the range of dispersion or the maximum phase velocity of extensional waves in composite rods consisting of an isotropic core and isotropic casing are discussed. A model of the maximum phase velocity of the extensional wave in a rod consisting of an isotropic core and transversely isotropic casing is developed. It is found that the maximum phase velocity of this system can be controlled within two bounding velocities. The frequency spectra of the extensional waves for several cases are developed, and the dispersion characteristics are discussed.

14. SUBJECT TERMS

Bar Wave Velocity, Dispersion, Composite Rod, Isotropic Core, Extensional Wave, Phase Velocity, Transversely Isotropic Casing

15. NUMBER OF PAGES

58

16. PRICE CODE

17. SECURITY CLASSIFICATION OF REPORT	18. SECURITY CLASSIFICATION OF THIS PAGE	19. SECURITY CLASSIFICATION OF ABSTRACT	20. LIMITATION OF ABSTRACT
UNCLASSIFIED	UNCLASSIFIED	UNCLASSIFIED	SAR

TABLE OF CONTENTS

LIST OF ILLUSTRATIONS

LIST OF TABLES

CONTROLLED DISPERSION OF THE EXTENSIONAL WAVE IN COMPOSITE ISOTROPIC AND TRANSVERSELY ISOTROPIC RODS

INTRODUCTION AND BACKGROUND

OBJECTIVE AND OVERVIEW

The objective of this work is to investigate the dispersion of extensional waves in composite isotropic and transversely isotropic rods. In particular, we are interested in the material and physical parameters that control the maximum and minimum phase velocities of the extensional wave.

We begin by developing the equations of motion of an infinitely long, layered rod with a transversely isotropic core and a transversely isotropic casing using the three-dimensional equations of elasticity. The equations of motion, which are general in axial wavenumber k and circumferential wavenumber n, are then specialized to the case of the $n = 0$ axisymmetric modes of wave propagation. Simplifications to these equations for the case of material isotropy are presented.

A model of the maximum phase velocity of the extensional waves in composite isotropic rods is discussed. It is found that, for a given set of material parameters, this maximum phase velocity is a function of the ratio of the outer radius of the casing and the radius of the core.

The extensional wave is dispersive, and as wavenumber increases to infinity the extensional wave phase velocity asymptotically approaches a minimum. This minimum velocity depends on the material parameters of the core and casing but is independent of system geometry. The ratio of the maximum phase velocity to the minimum phase velocity is the range of dispersion of the system.

Methodologies for controlling either the maximum phase velocity of the extensional wave or the range of dispersion in composite rods of isotropic materials are presented. The frequency spectrum of the extensional wave for four cases of an isotropic core and casing are developed, and

the dispersion characteristics are discussed.

Finally, dispersion of a composite rod consisting of an isotropic core and transversely isotropic casing is investigated. The transversely isotropic casing is a fiber-reinforced composite material. A model of the maximum phase velocity of the extensional waves in the system is developed and compared to the model for composite isotropic rods. Because of a priori assumptions of the dynamic behavior of the transversely isotropic casing, the asymptotic minimum phase velocity of the extensional wave cannot be investigated.

The frequency spectrum of the extensional wave in a rod with an isotropic core and transversely isotropic matrix is developed and compared to that of a composite isotropic rod. The isotropic core of both rods is identical. The transversely isotropic casing consists of a matrix material that is identical to the casing of the composite isotropic rod. The geometries of each system are selected so that the maximum phase velocity of the extensional wave in each rod is identical. The characteristics of the dispersion of the extensional wave in the two rods are discussed.

PREVIOUS INVESTIGATIONS

Beginning with the work of Pochhammer (1876) and Chree (1889), the modes of wave propagation in a homogeneous isotropic circular rod have been investigated in considerable detail. A concise discussion of the frequency spectrum of circular rods can be found in Achenbach (1987). Dispersion of axisymmetric modes in composite elastic rods has been investigated by McNiven et al. (1963), Armenakas (1965), Mengi and McNiven (1967), McNiven and Mengi (1967), and Lai (1971). However, in all of these investigations, the composite rod consisted of an isotropic core and an isotropic cladding.

A limited number of investigations exists in the area of wave propagation in cylinders composed of anisotropic materials, particularly based on the three-dimensional theory of elasticity. Chree (1890) may have been the first investigator of axisymmetric wave propagation in an anisotropic bar. In his analysis, the equations of motion of a transversely isotropic bar of any cross

2

section were developed and then specialized for the case of a circular rod. Approximate solutions were obtained by expanding the displacements in powers of the radius r. Later, Morse (1954) developed the exact solution of the problem studied by Chree (1890) and showed that the solution reduced to the Pochhammer solution for the isotropic case. No numerical results were presented by either Chree (1890) or Morse (1954). Mirsky (1965a, b) investigated axisymmetric and nonaxisymmetric wave propagation in transversely isotropic cylinders and used displacement potentials to solve the equations of motion. All the above investigations were for a rod or a hollow cylinder, but not a layered rod.

To the author's knowledge, the case of wave propagation in a composite rod consisting of an isotropic core and a transversely isotropic casing has not been investigated to date.

TRANSVERSELY ISOTROIC MATERIALS

Many natural and artificial materials are transversely isotropic. For example, hexagonal crystals (including beryllium, cadmium, magnesium, titanium, and zinc) are transversely isotropic. Ice is also transversely isotropic.

A unidirectional, fiber-reinforced composite material is transversely isotropic. This type of material is highly anisotropic because the stiffness and strength in the fiber direction are of the order of the values for the fiber, and are thus very high, while the stiffness and strength transverse to the fiber direction are of the order of the values for the matrix, and are thus much lower. Carbon and graphite, which are often used in fiber-reinforced materials, are themselves transversely isotropic.

The constitutive behavior of transversely isotropic materials is characterized by five independent elastic moduli. At every point in such materials, there exists a plane of isotropy in which the elastic moduli of the material are equal in all directions. The unit vector normal to the special plane of isotropy in a transversely isotropic material is called the preferred direction of the material. Comprehensive discussions of material symmetry and elastic moduli can be found in Jones (1975), Christensen (1979), and Sokolnikoff (1987).

3

WAVE PROPAGATION IN COMPOSITE BODIES AND COMPOSITE MATERIALS

A composite body consists of two or more materials that are macroscopically distinct and are joined together in order to achieve some useful property. The frequency equation of a composite body is developed from the imposed boundary conditions. If there are no a priori assumptions of the behavior of the system, which restrict investigations (e.g., to low wavenumbers), the frequency spectra of the modes of wave propagation in a composite body can be developed for all wavenumbers. This is not true for wave propagation in a composite material.

In a composite material, it is possible to define a representative volume element (Hashin, 1983). Representative volume elements are large compared to the dimensions of the components of the material. A necessary characteristic of a composite material is statistical homogeneity. In a statistically homogeneous composite material, all global characteristics (such as volume fractions, two-point correlations, etc.) are the same in any representative volume element, irrespective of its position within the material.

The *effective* elastic constants of a composite material are used to define the relations between the averages of field variables, such as stress and strain. The classical approach in the analysis of homogeneous composite materials is to assume that the field equations of elasticity are valid, with the effective properties of the composite material replacing the usual elastic properties of a homogeneous continuum.

Wave propagation in deformable composite materials can be broadly divided into two categories (Christensen, 1979). If the wavelength of the response of the material is long compared to the scale of the representative volume element, the material response is governed by the effective properties of the material. In this case, the equations of motion for the composite material are identical to those for homogeneous materials. If the wavelength of the response is not ideally long with respect to the representative volume element, very complicated dynamic effects occur. These effects include wave reflection and refraction at the interfaces of the components of the composite material. These phenomena are most important in the field of ultrasonics.

In this investigation, we assume that the dynamic behavior of the composite material is governed by the effective properties. As a result, the range in wavenumber for which we can develop the frequency spectra is limited.

ANALYTICAL FORMULATION

SYSTEM GEOMETRY AND APPROACH

The system under consideration is shown in figure 1. It consists of an infinitely long composite rod with a solid core of radius a and a casing of outer radius b. The system is assumed to be linear so that the linearized, three-dimensional stress equations of motion can be used. The system displacements and stresses are defined by the cylindrical coordinates, r, θ, and z. The cylindrical coordinate directions are designated as the 1, 2, and 3 directions, respectively.

We begin by assuming that the core and casing are composed of differing transversely isotropic materials. Each material has a preferred material direction collinear with the longitudinal axis of the cylinder. The equations of displacement and surface stress are presented as functions of geometry and material parameters. Simplifications of these equations (due to specializing either the core, the casing, or both, to the case of isotropy) are discussed.

The frequency equation of the system is then developed from the assumptions of (1) continuity of displacements and stresses at the interface between the core and casing and (2) a traction-free boundary condition on the surface of the rod.

DISPLACEMENTS AND STRESSES IN A COMPOSITE ROD

Solutions to the equations of motion of transversely isotropic cylinders were developed in a previous report (Berliner, 1995). The resulting displacements and stresses are repeated here but in a more general form to allow for systems consisting of multiple layers.

The displacement components are

Figure 1. System Geometry

$$_j u_r(r, \theta, z, t) = \{A_{1j} J_n(_j\zeta_1 r)_{,r} + B_{1j} Y_n(_j\zeta_1 r)_{,r}$$

$$+ A_{2j} J_n(_j\zeta_2 r)_{,r} + B_{2j} Y_n(_j\zeta_2 r)_{,r} \tag{1}$$

$$+ \frac{n}{r}[A_{3j} J_n(_j\zeta_3 r) + B_{3j} Y_n(_j\zeta_3 r)]\} \cos(n\theta) e^{-i(\omega t - kz)},$$

$$_j u_\theta(r, \theta, z, t) = \{-\frac{n}{r}[A_{1j} J_n(_j\zeta_1 r) + B_{1j} Y_n(_j\zeta_1 r)]$$

$$-\frac{n}{r}[A_{2j} J_n(_j\zeta_2 r) + B_{2j} Y_n(_j\zeta_2 r)] \tag{2}$$

$$-[A_{3j} J_n(_j\zeta_3 r)_{,r} + B_{3j} Y_n(_j\zeta_3 r)_{,r}]\} \sin(n\theta) e^{-i(\omega t - kz)},$$

and

$$_j u_z(r, \theta, z, t) = \{_j\eta_1[A_{1j} J_n(_j\zeta_1 r) + B_{1j} Y_n(_j\zeta_1 r)]$$

$$\tag{3}$$

$$+ _j\eta_2[A_{2j} J_n(_j\zeta_2 r) + B_{2j} Y_n(_j\zeta_2 r)]\} \cos(n\theta) e^{-i(\omega t - kz)},$$

and the surface stresses are

$$_j\tau_{rr} = \{2\,_jc_{66}\frac{n}{r}\left(A_{3j} J_n(_j\zeta_3 r)_{,r} + B_{3j} Y_n(_j\zeta_3 r)_{,r} - \frac{1}{r}[A_{3j} J_n(_j\zeta_3 r)\right.$$

$$+ B_{3j} Y_n(_j\zeta_3 r)]) - 2\frac{_jc_{66}}{r}[A_{1j} J_n(_j\zeta_1 r)_{,r} + B_{1j} Y_n(_j\zeta_1 r)_{,r}$$

$$+ A_{2j} J_n(_j\zeta_2 r)_{,r} + B_{2j} Y_n(_j\zeta_2 r)_{,r}] + 2\,_jc_{66}\frac{n^2}{r^2}[A_{1j} J_n(_j\zeta_1 r) + B_{1j} Y_n(_j\zeta_1 r) \tag{4}$$

$$+ A_{2j} J_n(_j\zeta_2 r) + B_{2j} Y_n(_j\zeta_2 r)] + \left(i\,_jc_{13}\,_j\eta_1 k - _jc_{11}\,_j\zeta_1^2\right)[A_{1j} J_n(_j\zeta_1 r)$$

$$+ B_{1j} Y_n(_j\zeta_1 r)] + \left(i\,_jc_{13}\,_j\eta_2 k - _jc_{11}\,_j\zeta_2^2\right)\left[A_{2j} J_n(_j\zeta_2 r) + B_{2j} Y_n(_j\zeta_2 r)\right]\}$$

$$\cos(n\theta) e^{-i(\omega t - kz)},$$

$$_j\tau_{zr} = {_jc_{44}} \{ ({_j}\eta_1 + ik) [A_{1j} J_n ({_j}\zeta_1 r)_{,r} + B_{1j} Y_n ({_j}\zeta_1 r)_{,r}]$$

$$+ ({_j}\eta_2 + ik) [A_{2j} J_n ({_j}\zeta_2 r)_{,r} + B_{2j} Y_n ({_j}\zeta_2 r)_{,r}] \tag{5}$$

$$+ ik\frac{n}{r} [A_{3j} J_n ({_j}\zeta_3 r) + B_{3j} Y_n ({_j}\zeta_3 r)] \} \cos(n\theta) e^{-i(\omega t - kz)},$$

and

$$_j\tau_{r\theta} = {_jc_{66}} \{ 2\frac{n}{r^2} [A_{1j} J_n ({_j}\zeta_1 r) + B_{1j} Y_n ({_j}\zeta_1 r) + A_{2j} J_n ({_j}\zeta_2 r) + B_{2j} Y_n ({_j}\zeta_2 r)]$$

$$-2\frac{n}{r} [A_{1j} J_n ({_j}\zeta_1 r)_{,r} + B_{1j} Y_n ({_j}\zeta_1 r)_{,r} + A_{2j} J_n ({_j}\zeta_2 r)_{,r} + B_{2j} Y_n ({_j}\zeta_2 r)_{,r}]$$

$$+ {_j}\zeta_3^2 \left[A_{3j} J_n ({_j}\zeta_3 r) + B_{3j} Y_n ({_j}\zeta_3 r) \right] + \frac{2}{r} [A_{3j} J_n ({_j}\zeta_3 r)_{,r} + B_{3j} Y_n ({_j}\zeta_3 r)_{,r}] \tag{6}$$

$$-2\frac{n^2}{r^2} \left[A_{3j} J_n ({_j}\zeta_3 r) + B_{3j} Y_n ({_j}\zeta_3 r) \right] \} \sin(n\theta) e^{-i(\omega t - kz)},$$

where the subscript j indicates the components and properties pertaining to layer j; n is the circumferential wavenumber; $i = \sqrt{-1}$; k is the axial wavenumber; ω is the radian frequency; J_n and Y_n are Bessel functions of order n of the first and second kind, respectively; and $J_n (\zeta_1 r)_{,r}$ denotes $\partial J_n (\zeta_1 r)/\partial r$, etc. In this investigation, $j = 1$ is used to indicate properties and components pertaining to the solid core, and $j = 2$ is used to indicate properties and components pertaining to the casing. Also, for finiteness of displacements and stresses at $r = 0$, the coefficients B_{11}, B_{21}, and B_{31} must be equal to zero.

The parameters in equations (1) through (6) are derived from the properties of the material as follows:

$$_j\zeta_1^2 = \frac{-_jB - \sqrt{_jB^2 - 4\,_jA\,_jC}}{2\,_jA},$$

$$_j\zeta_2^2 = \frac{-_jB + \sqrt{_jB^2 - 4\,_jA\,_jC}}{2\,_jA}, \tag{7}$$

$$_j\zeta_3^2 = \frac{\left(_j\rho\omega^2 - _jc_{44}k^2\right)}{_jc_{66}},$$

and

$$_j\eta_1 = \frac{ik\,_j\zeta_1^2\,(_jc_{13} + _jc_{44})}{\left(_j\rho\omega^2 - _jc_{33}k^2 - _jc_{44}\,_j\zeta_1^2\right)},$$

$$\tag{8}$$

$$_j\eta_2 = \frac{i\left(-_jc_{44}k^2 + _j\rho\omega^2 - _jc_{11}\,_j\zeta_2^2\right)}{(_jc_{13} + _jc_{44})\,k},$$

where

$$_jA = (_jc_{11}\,_jc_{44}),$$

$$_jB = -\left[(_jc_{11} + _jc_{44})\,_j\rho\omega^2 + \left(_jc_{13}^2 + 2\,_jc_{13}\,_jc_{44} - _jc_{11}\,_jc_{33}\right)k^2\right], \tag{9}$$

$$_jC = \left(_j\rho\omega^2 - _jc_{33}k^2\right)\left(_j\rho\omega^2 - _jc_{44}k^2\right),$$

and where $_j\rho$ is the density of the material and the coefficients $_jc_{11}$, $_jc_{12}$, etc., are the elastic constants of the material of layer j. These elastic constants are related to the more familiar engineering constants as

$$_jc_{11} = _jB_T + _jG_T,$$

$$_jc_{12} = _jB_T - _jG_T,$$

$$_jc_{13} = 2 \, _jB_T \, _jv_L,$$

$$_jc_{33} = _jE_L + 4 \, _jB_T \, _jv_L^2,$$

$$_jc_{44} = _jG_L,$$

$$_jc_{66} = (_jc_{11} - _jc_{12})/2, = _jG_T,$$

(10)

where

$_jB_T$ = the transverse bulk modulus,

$_jG_L$ = the longitudinal shear modulus,

$_jG_T$ = the transverse shear modulus,

$_jE_L$ = the longitudinal Young's modulus,

$_jE_T$ = the transverse Young's modulus,

$_jv_L$ = the longitudinal Poisson's ratio,

$_jv_T$ = the transverse Poisson's ratio.

"Transverse" refers to properties in the plane of isotropy and "longitudinal" refers to properties along the material preferred direction.

Effective Engineering Constants for a Fiber-Reinforced Matrix Material

When the transversely isotropic material is a fiber-reinforced matrix material, $_jc_{11}$, $_jc_{12}$, etc., are the effective *elastic* constants of the material. These effective elastic constants are defined from effective engineering constants. For this investigation, we use the definitions for the effective *engineering* constants derived by Jones (1975) as follows:

12

$$_jG_T = \frac{_jE_T}{2\left(1 + {}_j\nu_T\right)},$$

$$_jG_L = \frac{\left({}_jG_m\, {}_jG_f\right)}{\left({}_jV_m\, {}_jG_f + {}_jV_f\, {}_jG_m\right)},$$

$$_jE_L = {}_jV_f\, {}_jE_f + {}_jV_m\, {}_jE_m,$$

$$_jE_T = \frac{\left({}_jE_m\, {}_jE_f\right)}{\left({}_jV_m\, {}_jE_f + {}_jV_f\, {}_jE_m\right)}, \qquad (11)$$

$$_j\nu_L = {}_jV_f\, {}_j\nu_f + {}_jV_m\, {}_j\nu_m,$$

$$_j\rho = {}_j\rho_f\, {}_jV_f + {}_j\rho_m\, {}_jV_m,$$

where $_jE_m$, $_jG_m$, $_j\nu_m$, $_j\rho_m$, and $_jV_m$ are the Young's modulus, shear modulus, Poisson's ratio, density, and volume fraction of the matrix material of layer j, respectively, and where $_jE_f$, $_jG_f$, $_j\nu_f$, $_j\rho_f$, and $_jV_f$ are the Young's modulus, shear modulus, Poisson's ratio, density, and volume fraction of the fiber of layer j, respectively. The transverse bulk modulus of each layer is defined by Hashin (1979) as

$$2\,_j\beta_T = \frac{_jE_T}{1 - {}_j\nu_T - 2\, {}_j\nu_2^L\, \dfrac{_jE_T}{_jE_L}}. \qquad (12)$$

Specialized Case of Isotropy

We can specialize the constitutive behavior of the core or the casing from transversely isotropic to isotropic by reducing the number of elastic constants from five to two using the following relationships:

$$_j c_{33} = {}_j c_{11},$$

$$_j c_{13} = {}_j c_{12},$$

$$_j c_{44} = {}_j c_{66} = \frac{({}_j c_{11} - {}_j c_{12})}{2}. \tag{13}$$

These elastic constants are written in terms of the engineering constants (also known as technical constants) of the material as follows:

$$_j c_{11} = \frac{{}_j E\,(1 - {}_j v)}{(1 + {}_j v)\,(1 - 2\,{}_j v)},$$

$$_j c_{12} = \frac{{}_j E\,{}_j v}{(1 + {}_j v)\,(1 - 2\,{}_j v)}, \tag{14}$$

$$_j c_{44} = \frac{{}_j E}{2\,(1 + {}_j v)},$$

where $_j E$ is the Young's modulus and $_j v$ is the Poisson's ratio of the material. By normalizing $_j c_{11}$ and $_j c_{12}$ to $_j c_{44}$, these elastic constants simplify to

$$_j c_{11} = \frac{2\,(1 - {}_j v)}{(1 - 2\,{}_j v)}\,{}_j c_{44},$$

$$_j c_{12} = \frac{2\,{}_j v}{(1 - 2\,{}_j v)}\,{}_j c_{44}. \tag{15}$$

Substitution of equations (13) and (15) into equations (7) and (8) results in the following simplifications:

$$_j\zeta_1^2 \rightarrow \frac{j\rho\omega^2}{{}_jc_{44}} - k^2,$$

$$_j\zeta_2^2 \rightarrow \frac{j\rho\omega^2}{{}_jc_{11}} - k^2,$$

$$_j\zeta_3^2 \rightarrow \frac{j\rho\omega^2}{{}_jc_{44}} - k^2 = {}_j\zeta_1^2, \tag{16}$$

$$ik\,{}_j\eta_1 \rightarrow \frac{j\rho\omega^2}{{}_jc_{44}} - k^2,$$

$$ik\,{}_j\eta_2 \rightarrow -k^2.$$

BOUNDARY CONDITIONS

To complete the analytical formulation of the frequency equation of the system requires consideration of the boundary conditions. At the solid-solid interface, $r = a$, the continuity conditions require that the three displacement components and the three surface stress components for the core and casing be equal (Fung, 1977). The traction-free boundary condition on the outer surface of the composite rod requires that the three surface stress components are zero at $r = b$.

These boundary conditions can be written as

$$\left[{}_1\tau_{rr},\ {}_1\tau_{zr},\ {}_1\tau_{r\theta},\ {}_1u_r,\ {}_1u_\theta,\ {}_1u_z\right]_{r=a} = \left[{}_2\tau_{rr},\ {}_2\tau_{zr},\ {}_2\tau_{r\theta},\ {}_2u_r,\ {}_2u_\theta,\ {}_2u_z\right]_{r=a} \tag{17}$$

and

$$\left[{}_2\tau_{rr},\ {}_2\tau_{zr},\ {}_2\tau_{r\theta}\right]_{r=b} = [0, 0, 0]_{r=b}. \tag{18}$$

Equations (17) and (18) represent a system of nine linear algebraic equations in unknown wave amplitudes that, in matrix form, are

$$[L_{p,q}]\ \{c\} = \{0\} \qquad (p = 1, 2, \ldots 9; q = 1, 2, \ldots 9), \tag{19}$$

where $[L_{p,q}]$ is a 9-by-9 matrix whose components are found from equations (1) through (6) and

where $\{c\}$ is a 9-by-1 column vector of the unknown amplitude coefficients A_{11}, A_{21}, A_{31}, A_{12}, B_{12}, A_{22}, B_{22}, A_{32}, and B_{32}. The components of $[L_{p,q}]$ are defined in appendix A.

The solution of equation (19) is nontrivial when the determinant of the coefficients of the wave amplitudes $\{c\}$ vanishes, i.e., when,

$$\left|L_{p,q}\right| = 0. \tag{20}$$

Equation (20) is the frequency equation of the system. When the material and geometrical parameters are given, equation (20) yields an implicit transcendental relationship between wavenumber and frequency.

NUMERICAL ANALYSIS

FREQUENCY EQUATION FOR AXISYMMETRIC MODES

We begin by specializing the coupled system for the case of the $n = 0$ axisymmetric modes of wave propagation. When $n = 0$, the displacements of the system are independent of θ. The motions separate into torsional modes consisting of $_j u_\theta$ (r, θ, z, t) only and into longitudinal modes consisting of $_j u_r$ (r, θ, z, t) and $_j u_z$ (r, θ, z, t). In this investigation, we restrict our results to longitudinal modes of the system.

When $n = 0$, many of the components of the matrix $[L_{p, q}]$ become equal to zero, and as a result, equation (20) separates into the product of the two subdeterminants

$$Det_1 Det_2 = 0, \tag{21}$$

where

$$Det_1 = |L_{p, q}| \qquad (p = 1, 2, 4, 6, 7, 8; q = 1, 2, 3, 4, 7, 8) \tag{22}$$

and

$$Det_2 = |L_{p, q}| \qquad (p = 3, 5, 9; q = 5, 6, 9). \tag{23}$$

The components of the determinants are defined in appendix A, with $n = 0$.

Equation (21) is satisfied if either Det_1 or Det_2 is equal to zero. The case $Det_1 = 0$ is the frequency equation for axisymmetric longitudinal modes in a composite rod. The case $Det_2 = 0$ is the frequency equation for axisymmetric torsional modes in a composite rod. Since only the longitudinal modes are of interest, we will only seek solutions to

$$Det_1 = 0. \tag{24}$$

SOLUTIONS OF THE FREQUENCY EQUATION FOR LONGITUDINAL MODES

The arguments of the Bessel functions in equation (24) can be real, imaginary, or complex. Therefore, equation (24) is a complex algebraic equation. Solution of this equation requires that the real and imaginary parts vanish simultaneously. For any wavenumber, there are an infinite number of frequencies that are solutions to equation (24). Typically, root searches for each branch of the spectrum begin at a cutoff frequency. The wavenumber is then increased by a small increment and the search for the next root is conducted within the neighborhood of the previous root. This process is repeated over the wavenumber band of interest. Spurious roots can also occur at the frequencies where arguments of the Bessel functions vanish. These roots can be determined in advance and eliminated from the frequency spectrum. The root searches were conducted using Mueller's method (Press et al., 1986). Mueller's method is an algorithm that finds a real or complex zero of a complex function, which in this case is equation (24).

COMPUTATIONAL RESULTS

The extensional wave is the lowest and is commonly accepted to be the most important longitudinal mode (Achenbach, 1987; McNiven and Mengi, 1967). This mode is characterized by primarily axial displacements. In this investigation, we limit the following computational results to the extensional wave.

These results are discussed as functions of normalized frequency Ω, normalized wavenumber δ, normalized phase velocity $\hat{c}$, and the ratio of b to a, where these normalized variables are defined as

a = radius of core,

b = outer radius of casing,

$R = \dfrac{b}{a}$,

$\Omega = \dfrac{\omega a}{{}_1 c_B}$, normalized frequency,

$\delta = ka$, normalized wavenumber,

$\hat{c} = \dfrac{\Omega}{\delta}$, normalized phase velocity,

and where

$$
{}_1 c_B = \sqrt{\frac{{}_1 E}{{}_1 \rho}} \qquad\qquad (25)
$$

is the bar wave velocity in the core of the composite rod (Achenbach, 1987). Using the root search technique described above, the frequency spectrum was developed over real normalized wavenumbers from 0 to 0.1.

ISOTROPIC CORE AND ISOTROPIC CASING

The first cases to be investigated are composite rods consisting of an isotropic silica glass core and linear isotropic elastomeric casings. (Note that the material properties for all cases

investigated can be found in appendix B.)

Figure 2 is the frequency spectra of the extensional wave in a composite rod with a rubber casing and five values of R. Two comments can be immediately made about the behavior of these systems as functions of R and of δ: (1) As R increases, the normalized phase velocity $\hat{c}$ decreases over all normalized wavenumbers and (2) For any R, the normalized phase velocity as $\delta \to 0$ is different from the normalized phase velocity as $\delta \to \infty$. Because the phase velocity of the extensional wave is not constant with wavenumber, it is dispersive.

The larger the range of phase velocities, the more dispersive is the extensional wave. McNiven and Mengi (1967) established the extent of this range, as functions of geometry and material properties, by defining the velocities bounding the frequency spectrum of this mode.

Maximum Phase Velocity of the Extensional Wave

Using the classical kinematic assumption that plane cross sections remain plane during deformation, McNiven and Mengi (1967) found that the maximum phase velocity associated with the extensional wave occurred when $k = 0$ and that this velocity was equal to the bar wave velocity of the composite rod. They defined this velocity as

$$c_B = \sqrt{\frac{E_{eff}}{\rho_{eff}}}, \tag{26}$$

where

$$E_{eff} = \frac{\left({}_1E_1A + {}_2E_2A \right)}{A} \tag{27}$$

and

$$E_{eff} = \frac{\left({}_1E_1A + {}_2E_2A \right)}{A}. \tag{28}$$

20
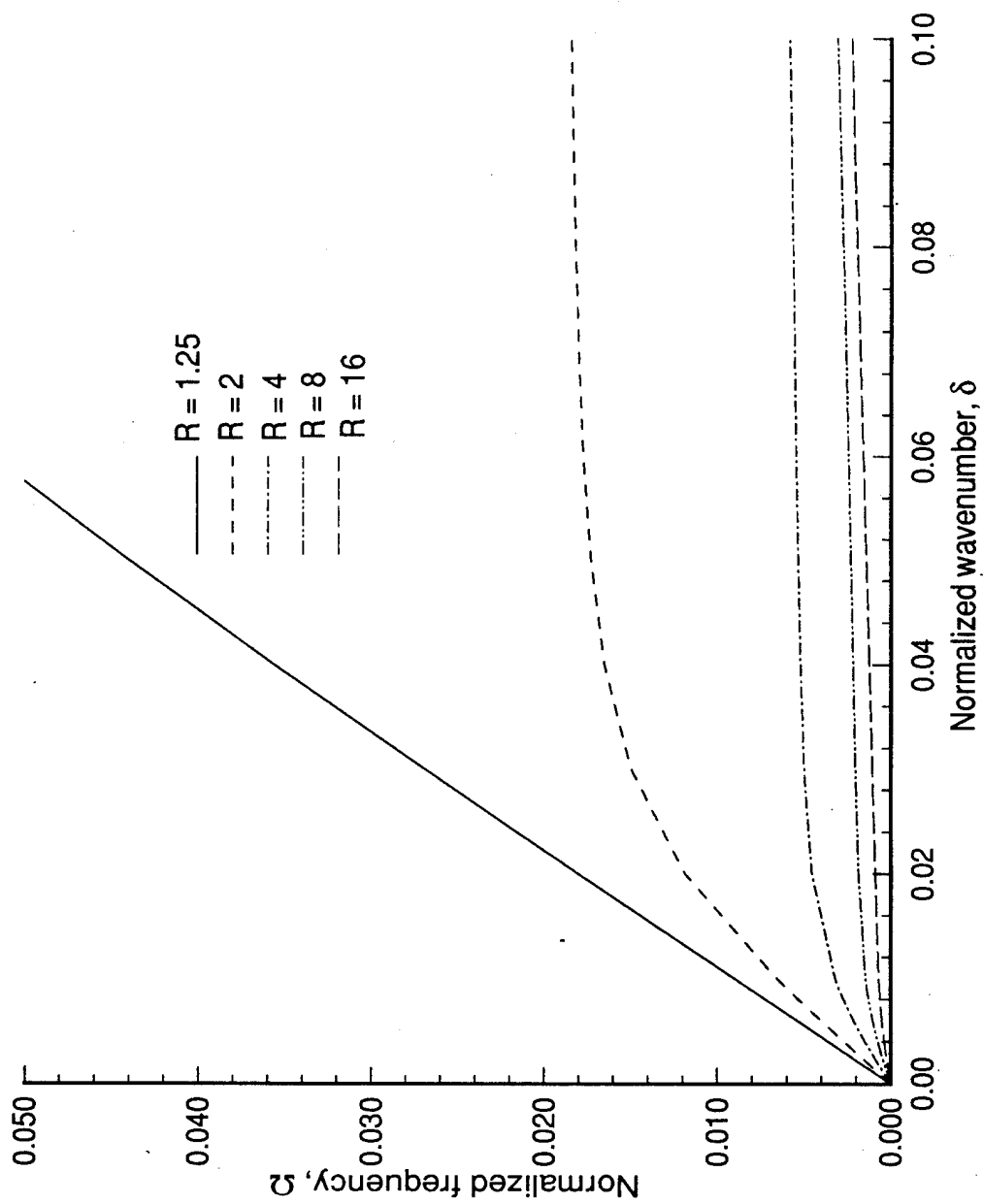
Figure 2. Frequency Spectra of Extensional Waves in Composite Rods With a Silica Glass Core and a Rubber Casing as a Function of R

R = 1.25
R = 2
R = 4
R = 8
R = 16

Normalized wavenumber, δ

Normalized frequency, Ω

In equation (28), E_{ff} is the effective Young's modulus of the composite rod, ρ_{eff} is the effective density of the rod, $_1A$ is the cross-sectional area of the core, $_2A$ is the cross-sectional area of the casing, and A is the total cross-sectional area of the rod. Equations (27) and (28) are sometimes called a "rule of mixtures" (Jones, 1975). Lai (1971) later derived equation (26) from the exact frequency equation by using low argument approximations for the Bessel functions.

We can put equation (26) in a more convenient form by rearranging and substituting $_1A = \pi a^2$, $_2A = \pi\left(b^2 - a^2\right)$, and $R = (b/a)$, resulting in

$$c_B = \sqrt{\frac{_1E}{_1\rho}} \sqrt{\frac{\frac{_2E}{_1E}\left(1 - \frac{1}{R^2}\right) + \frac{1}{R^2}}{\frac{_2\rho}{_1\rho}\left(1 - \frac{1}{R^2}\right) + \frac{1}{R^2}}}$$

(29)

$$= {_1c_B} \sqrt{\frac{\frac{_2E}{_1E}\left(1 - \frac{1}{R^2}\right) + \frac{1}{R^2}}{\frac{_2\rho}{_1\rho}\left(1 - \frac{1}{R^2}\right) + \frac{1}{R^2}}}.$$

Inspection of equation (29) shows that the *maximum* phase velocity of the extensional wave in the composite rod is bounded by the phase velocity of the bar wave in the core as $R \rightarrow 1$ and by the phase velocity of the bar wave in the casing as $R \rightarrow \infty$, where the bar wave velocity in the casing is defined by

$$_2c_B = \sqrt{\frac{_2E}{_2\rho}}.$$

(30)

In the case of a silica glass core with a rubber casing, the phase velocity of the bar wave in the casing is less than the phase velocity of the bar wave in the core. Therefore, $\sqrt{_1E/_1\rho}$ is the upper bound and $\sqrt{_2E/_2\rho}$ is the lower bound of the *maximum* phase velocity of the extensional

wave in the composite rod, and the phase velocity decreases as R increases, as was noted in figure 2. Figure 3 shows the same frequency spectra as figure 2 but only plotted to $\delta = 0.01$ and $\Omega = 0.01$ to emphasize the progressive reduction in phase velocity with increasing R and the nearly linear behavior of the extensional wave at low wavenumbers.

Minimum Phase Velocity of the Extensional Wave

The composite rods in this section represent composite bodies composed of two isotropic materials. As discussed earlier, since the frequency equation for this system is exact, the frequency spectra of the extensional wave can be developed over all wavenumbers. Therefore, we can analyze the behavior of these systems as $k \rightarrow 0$ (as was done above) and the asymptotic behavior of these systems as $k \rightarrow \infty$. Mengi and McNiven (1967) found that all axisymmetric waves in an infinitely long, composite rod, consisting of an isotropic core and an isotropic casing, asymptotically approach the phase velocity of certain classical waves as $k \rightarrow \infty$. These classical waves are Rayleigh waves in the casing, Stonely waves at the interface of the core and casing, and shear waves in the core or casing.

Composite rods of this geometry can be grouped into one of four classes. First, the rods are grouped into one of two classes determined by whether the shear wave velocity in the casing is faster or slower than the shear wave velocity in the core. The material in which the shear wave velocity is less is called the acoustically denser of the two materials. These two classes are each further subdivided into two classes, depending upon the ability of the composite rod to propagate Stonely waves at the interface. A brief description of these four classes, as well as the asymptotic phase velocity of the extensional wave for each class, is repeated in table 1 to aid the reader.
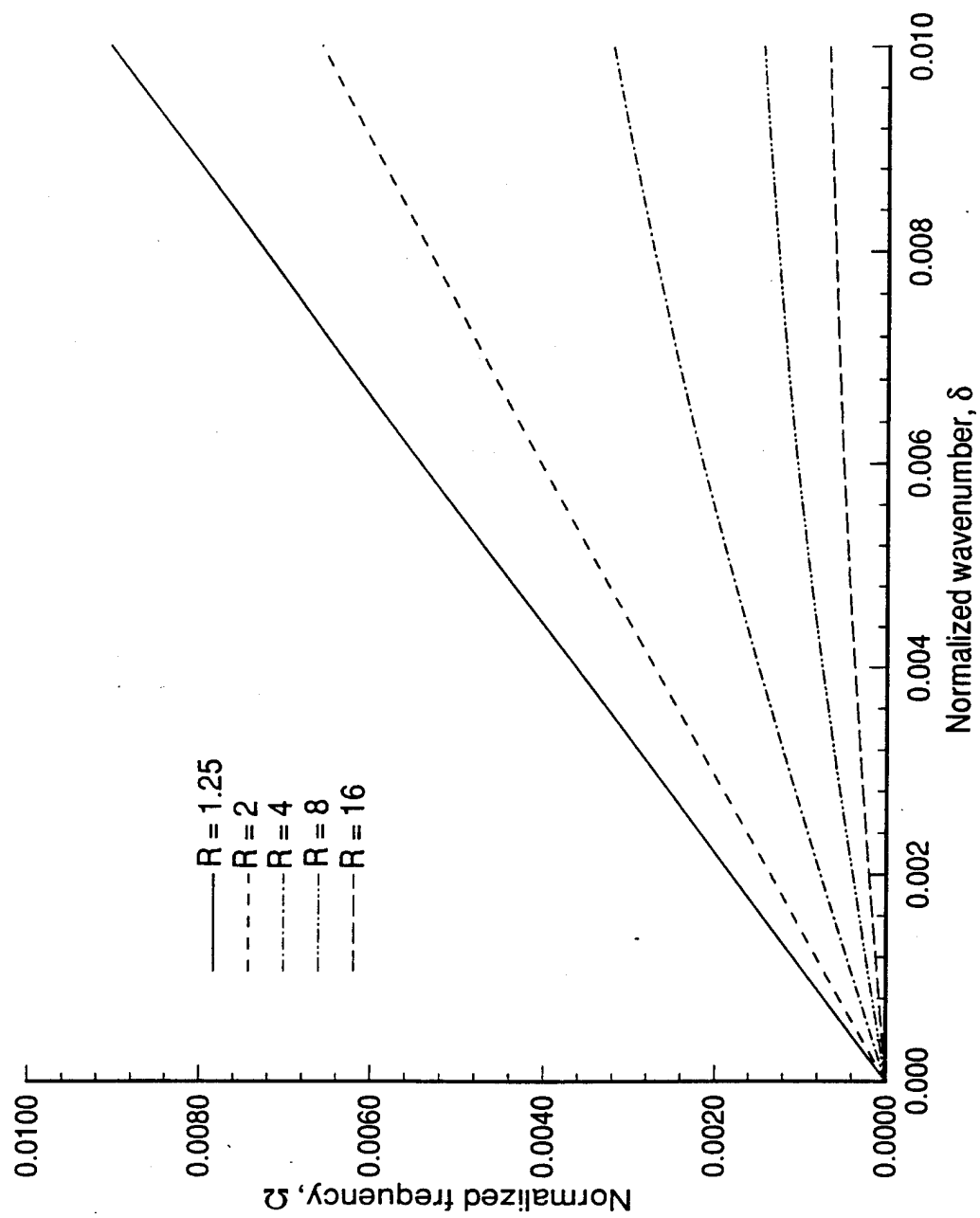
Figure 3. Low Wavenumber-Frequency Spectra of Extensional Waves in Composite Rods With a Silica Glass Core and a Rubber Casing as a Function of R

Table 1. Classes of Composite Rods

Class	Description
I	This rod has an acoustically dense core and the system propagates Stonely waves. The extensional wave velocity asymptotically approaches the Stonely velocity.
II	This rod also has an acoustically dense core but does not propagate Stonely waves. The extensional wave velocity asymptotically approaches the shear wave velocity in the core.
III	The casing of this rod is acoustically denser and the system propagates Stonely waves. The extensional wave asymptotically approaches the velocity of Rayleigh waves in the casing.
IV	This rod also has an acoustically dense casing but does not propagate Stonely waves. However, the extensional wave velocity in this type of rod also asymptotically approaches the velocity of Rayleigh waves in the casing, as it does in the Class III type of rods.

The frequency equation for Stonely waves is determined by the boundary conditions at the interface of two materials (Achenbach, 1987). Stonely waves will propagate at the interface of two materials only when the roots of this frequency equation are real. When Stonely waves do exist, they are nondispersive.

The composite rod of a silica glass core and a rubber casing is either Class III or Class IV because the shear wave velocity in the casing is slower than the shear wave velocity in the core. As noted above, the extensional wave velocity of either of these classes of composite rods asymptotically approaches the velocity of Rayleigh waves in the casing, regardless of whether the system propagates a Stonely wave or not. Therefore, we do not have to investigate the characteristics of the roots of the frequency equation for Stonely waves in this system.

The Rayleigh velocity in the casing is approximately given by

$$_2 c_R \cong \frac{(0.862 + 1.14 \,_2 v)}{(1 + \,_2 v)} \,_2 c_T , \qquad (31)$$

where

25

$$_2c_T = \sqrt{\frac{_2C_{44}}{_2\rho}} \tag{32}$$

is the shear wave velocity in the casing. Equation (31) represents the *minimum* phase velocity of the extensional wave in the composite rod. Contrary to the maximum phase velocity of the extensional wave, the minimum phase velocity of this system is independent of R. It is also interesting to note how this asymptotic behavior differs from that of a solid, one-material rod. For that case, Achenbach (1987) has shown that the phase velocity asymptotically approaches from below the velocity of Rayleigh waves and that at some intermediate wavenumber the phase velocity has a minimum value less than c_R.

Controlled Dispersion Characteristics of the Extensional Wave

McNiven and Mengi (1967) defined a *measure* of the dispersion of the extensional wave in a composite rod as the ratio of the two bounding velocities. This measure of dispersion is written as

$$H = \frac{c_0^2}{c_\infty^2}, \tag{33}$$

where c_0 is the maximum phase velocity and c_∞ is the minimum phase velocity. In the case under investigation, equation (29) defines the maximum phase velocity and equation (31) defines the minimum phase velocity, resulting in

$$H = \left(\frac{_1c_B}{_2c_T}\right)^2 \frac{\left(\frac{_2E}{_1E}\left(1 - \frac{1}{R^2}\right) + \frac{1}{R^2}\right)}{\left(\frac{_2\rho}{_1\rho}\left(1 - \frac{1}{R^2}\right) + \frac{1}{R^2}\right)} \frac{(1 + _2\nu)^2}{(0.862 + 1.14\,_2\nu)^2}. \tag{34}$$

Equations (29), (31), and (34) can be used to control the dispersion characteristics of the extensional wave in composite rods, as discussed below.

26

Controlling the <u>Maximum Phase Velocity</u> of the Extensional Wave. When the bar wave velocity of the casing is less than that in the core, the maximum phase velocity of the extensional wave in the composite rod is bounded by the bar wave velocity of the core (upper limit) and the bar wave velocity of the casing (lower limit). For a given set of properties for the core and casing, we can limit the maximum phase velocity, within these bounding velocities, by selecting R. Rearranging equation (29), we have

$$R = \sqrt{\frac{\left({}_1E - {}_2E - c_B^2 \, {}_1\rho + c_B^2 \, {}_2\rho \right)}{\left(c_B^2 \, {}_2\rho - {}_2E \right)}}. \qquad (35)$$

As an example of this procedure, we arbitrarily select a maximum phase velocity, c_B, of 1000 m/sec and determine the required value of R for four different casing materials, designated as "rubber," "lomod," "alcryn_low," and "alcryn_high," each with silica glass as the core material. As mentioned earlier, the properties for these materials are listed in appendix B. When the material properties and c_B = 1000 m/sec are substituted into equation (35), the following ratios of outer casing radius to core radius are found:

rubber: R = 8.45,
lomod: R = 9.37,
alcryn_low: R = 8.79,
alcryn_high: R = 8.46.

Using these values for R, along with the pertinent material properties, the frequency spectrum of the extensional wave was developed for each composite rod. Figure 4 is a plot of each of these spectra along with the line representing a constant normalized phase velocity of 1000 m/sec. It is apparent that, although the maximum phase velocity of each composite rod has been limited to 1000 m/sec, the range of dispersion is not the same. This is because the minimum phase velocity of each composite rod is different.

We use equation (31) to calculate the minimum phase velocity of each composite rod with the following results:
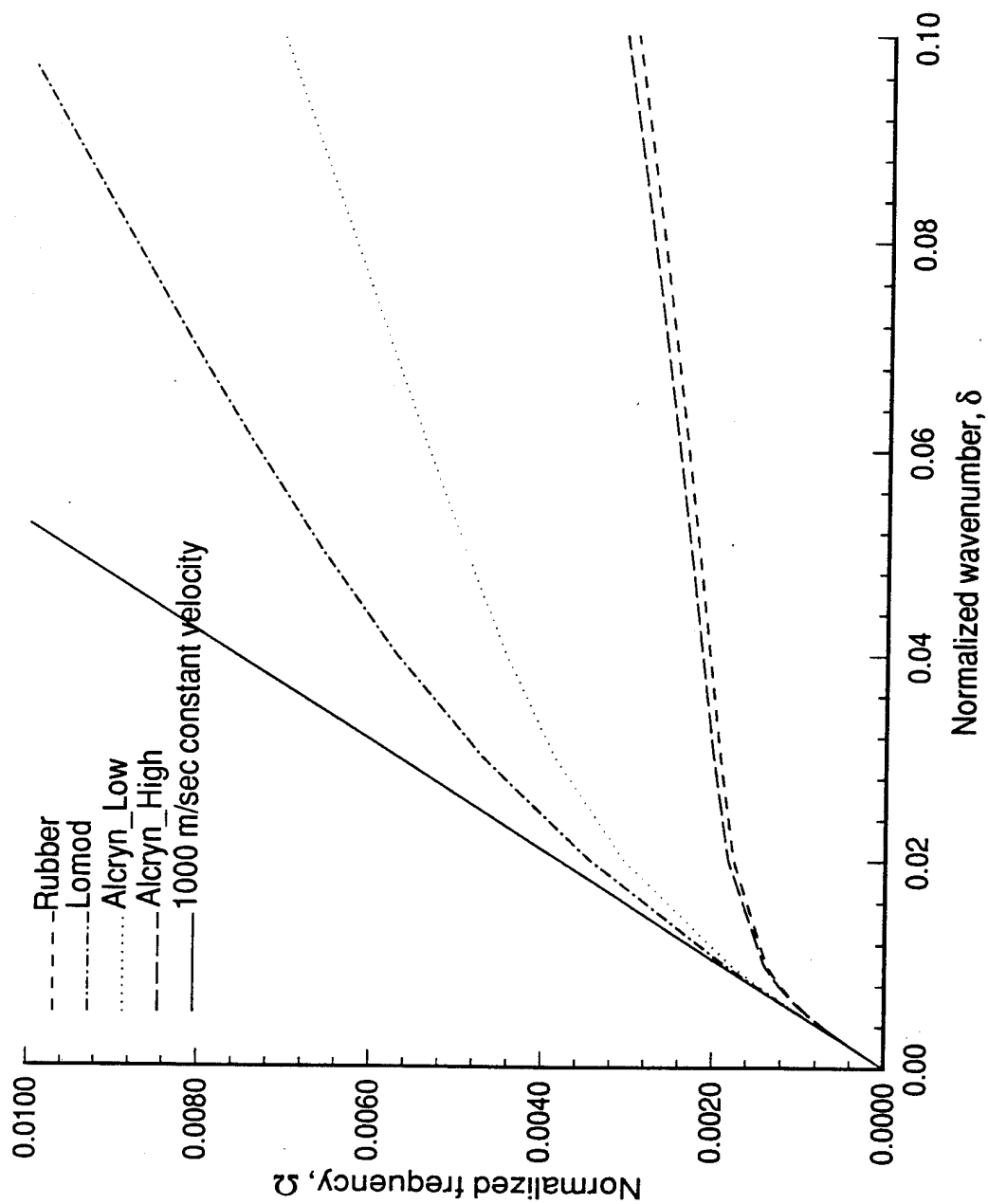
Figure 4. Frequency Spectra of Extensional Waves in Composite Rods With a Silica Glass Core and Casings of Four Different Materials

$$\text{rubber: } {}_2c_R \cong 68.19 \text{ m/sec,}$$

$$\text{lomod: } {}_2c_R \cong 251.61 \text{ m/sec,}$$

$$\text{alcryn\_low: } {}_2c_R \cong 167.98 \text{ m/sec,}$$

$$\text{alcryn\_high: } {}_2c_R \cong 71.31 \text{ m/sec.}$$

The range of dispersion can now be determined by substituting $c_0 = c_B = 1000$ m/sec and $c_\infty = {}_2c_R$ for each of the materials into equation (33) with the following results:

$$\text{rubber: } H \cong 215.06,$$
$$\text{lomod: } H \cong 15.8,$$
$$\text{alcryn\_low: } H \cong 35.44,$$
$$\text{alcryn\_high: } H \cong 196.65.$$

The larger the range of dispersion, H, the more dispersive is the composite rod (McNiven and Mengi, 1967) and the lower in wavenumber is the phase velocity of the extensional wave when it begins to deviate from the maximum. Inspection of the above calculations for H indicate that the composite rod with a casing of lomod material is the least dispersive and the composite rod with a casing of rubber is the most dispersive. This agrees with the results plotted in figure 4.

Figure 5 shows the same frequency spectra of figure 4 but plotted over a smaller wavenumber and frequency band. This figure emphasizes the nearly linear behavior of the extensional wave at the low wavenumbers and frequencies. The exact phase velocity of the extensional wave at $\delta = 0.01$ in each composite rod with the listed material as the casing material is

$$\text{rubber: } c \cong 717 \text{ m/sec,}$$
$$\text{lomod: } c \cong 973 \text{ m/sec,}$$
$$\text{alcryn\_low: } c \cong 936 \text{ m/sec,}$$
$$\text{alcryn\_high: } c \cong 734 \text{ m/sec.}$$

These results also confirm that the rod with the casing of lomod is the least dispersive and that, at $\delta = 0.01$, the phase velocity of the extensional wave is only approximately 2.7 percent less than the maximum phase velocity of 1000 m/sec. On the other hand, the rod with the casing of rubber
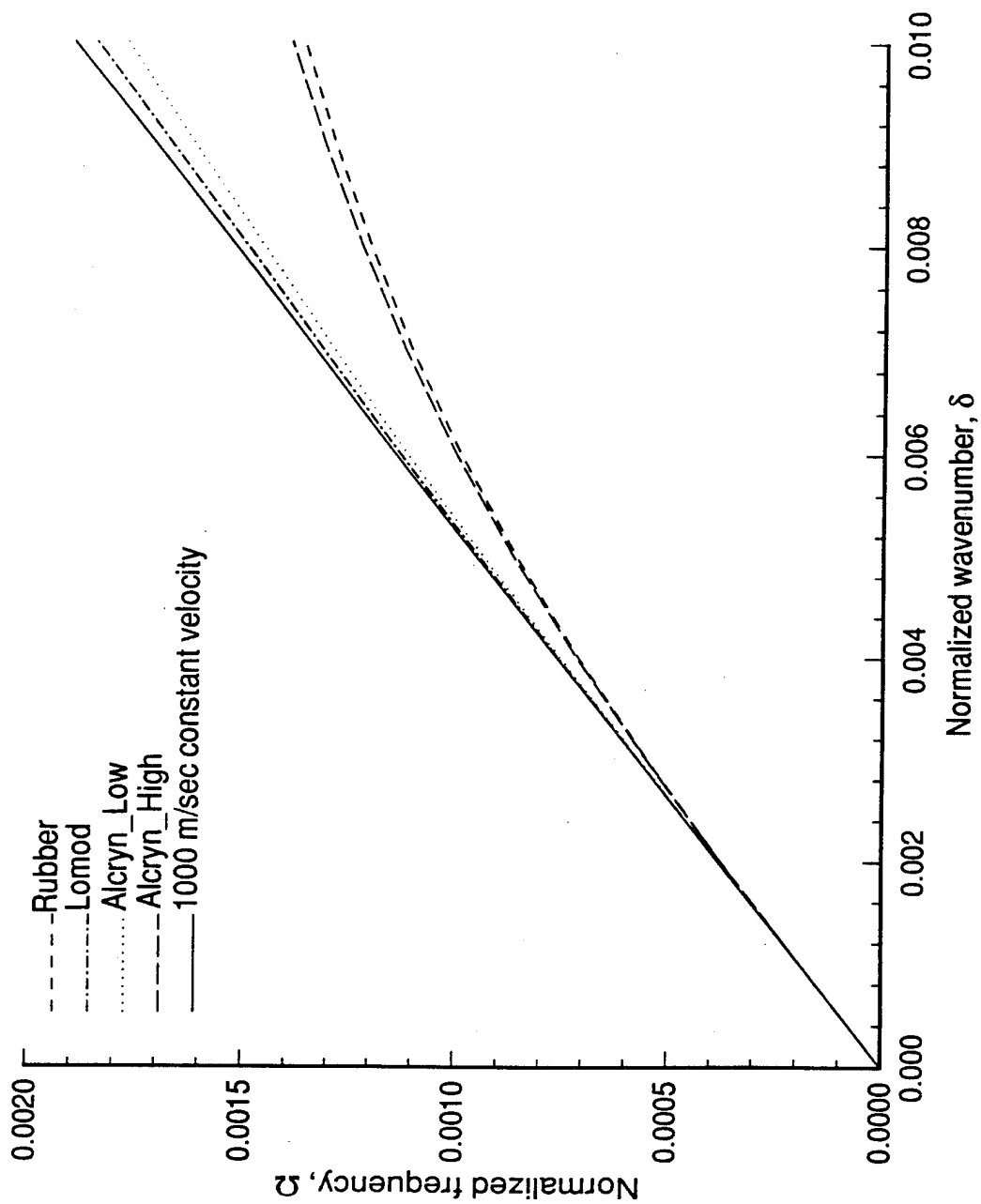
Figure 5. Low Wavenumber-Frequency Spectra of Extensional Waves in Composite Rods With a Silica Glass Core and Casings of Four Different Materials

is the most dispersive and, at $\delta = 0.01$, the phase velocity of the extensional wave is over 28 percent less than the maximum phase velocity.

Controlling the <u>Range of Dispersion</u> of the Extensional Wave. Instead of controlling the maximum phase velocity of the extensional wave in the composite rod, we may wish to control the range of dispersion. We can use equation (34) to solve for R for any desired H when given the material properties of the core and the casing. For example, if the casing material is rubber, and if the desired values of H are 10 or 100, the following values of R are required:

$$H = 10; R = 47.8,$$
$$H = 100; R = 12.7.$$

If the casing material is lomod, the following values of R are required for the same values of H:

$$H = 10; R = 12.9,$$
$$H = 100; R = 3.42.$$

Inspection of equation (34) shows that for any given material properties of the core and casing, there is a lower bound on H as $R \rightarrow \infty$. The lower bound for the composite rod with a rubber casing is $H = 3.22$, and the lower bound for the composite rod with a casing of lomod is $H = 3.16$.

ISOTROPIC CORE AND TRANSVERSELY ISOTROPIC CASING

The next case to be investigated is a composite rod consisting of an isotropic silica glass core and a transversely isotropic casing. The transversely isotropic casing consists of a fiber-reinforced rubber matrix with a preferred material direction collinear with the longitudinal axis of the rod. The matrix material has the same material properties as in the case of the composite rod with an isotropic rubber casing. The fibers are nylon and the fiber volume fraction is 10 percent. (The material properties of the matrix material and the nylon fibers are found in appendix B.)

When the material properties of the matrix material and of the reinforcing fibers, along with a 10-percent volume fraction of fiber, are substituted into equations (11) and (12), the effective

31

engineering constants of the transversely isotropic casing are found to be

$$_2B_T = 1.54 \times 10^7 \ \text{N/m}^2,$$

$$_2G_L = 5.75 \times 10^6 \ \text{N/m}^2,$$

$$_2G_T = 5.75 \times 10^6 \ \text{N/m}^2,$$

$$_2E_L = 5.64 \times 10^8 \ \text{N/m}^2,$$

$$_2E_T = 1.67 \times 10^7 \ \text{N/m}^2,$$

$$_2\nu_L = 0.42,$$

$$_2\nu_T = 0.45,$$

$$_2\rho = 1014 \ \text{kg/m}^3.$$

Substitution of the effective engineering constants into the definitions of the elastic constants (see equation (10)) results in

$$c_{11} = 2.12 \times 10^7 \ \text{N/m}^2,$$

$$c_{12} = 9.69 \times 10^6 \ \text{N/m}^2,$$

$$c_{13} = 1.3 \times 10^7 \ \text{N/m}^2,$$

$$c_{33} = 5.74 \times 10^8 \ \text{N/m}^2,$$

$$c_{44} = 5.74 \times 10^6 \ \text{N/m}^2,$$

$$c_{44} = 5.74 \times 10^6 \ \text{N/m}^2.$$

Maximum Phase Velocity of the Extensional Wave

In this section, we develop a low-wavenumber model of the maximum extensional wave velocity in this system based on the following assumptions:

1. We use the same classical kinematic assumption of McNiven and Mengi (1967). That is, we assume that plane cross sections remain plane during deformation and that the extensional wave

velocity at low wavenumbers is defined by equation (26) as

$$c_B = \sqrt{\frac{E_{eff}}{\rho_{eff}}}.$$

2. Since, at low wavenumbers, the extensional wave is characterized by primarily longitudinal displacements, we assume that the longitudinal Young's modulus $_2E_L$ and the density $_2\rho$ are the governing material properties of the casing for this mode. Therefore, we define the effective Young's modulus and the effective density of the composite rod as

$$E_{eff} = \frac{\left(_1E \, _1A + _2E_L \, _2A \right)}{A} \tag{36}$$

and

$$\rho_{eff} = \frac{\left(_1\rho \, _1A + _2\rho \, _2A \right)}{A}, \tag{37}$$

respectively.

When equations (36) and (37) are substituted into equation (26), along with $_1A = \pi a^2$, $_2A = \pi (b^2 - a^2)$, and $R = b/a$, the low-wavenumber model of the phase velocity of the extensional wave becomes

$$c_B = \sqrt{\frac{{}_1E}{{}_1\rho}} \sqrt{\frac{\left(\frac{2E_L}{{}_1E}\left(1 - \frac{1}{R^2}\right) + \frac{1}{R^2}\right)}{\left(\frac{2\rho}{{}_1\rho}\left(1 - \frac{1}{R^2}\right) + \frac{1}{R^2}\right)}}$$

(38)

$$= {}_1c_B \sqrt{\frac{\left(\frac{2E_L}{{}_1E}\left(1 - \frac{1}{R^2}\right) + \frac{1}{R^2}\right)}{\left(\frac{2\rho}{{}_1\rho}\left(1 - \frac{1}{R^2}\right) + \frac{1}{R^2}\right)}}.$$

The form of equation (38) is identical to equation (29) when ${}_2E$ is replaced by ${}_2E_L$. As in the case of a composite rod consisting of an isotropic core and casing, the *maximum* phase velocity of the extensional wave in this system is bounded by the phase velocity of the bar wave in the core as $R \rightarrow 1$ and by the phase velocity of the bar wave in the casing as $R \rightarrow \infty$, where the bar wave velocity in the casing is defined as

$$_2c_B = \sqrt{\frac{{}_2E_L}{{}_2\rho}}.$$

(39)

This bounding velocity depends on the volume fractions and properties of the matrix material and reinforcing fibers since from equation (11) we note

$$_jE_L = {}_jV_f\,{}_jE_f + {}_jV_m\,{}_jE_m.$$

(40)

Minimum Phase Velocity of the Extensional Wave

The composite rod in this section represents a composite body composed of an isotropic core and a transversely isotropic casing. Because the transversely isotropic casing consists of a composite material, assumptions regarding its dynamic behavior have been made a priori. That is, since we have assumed that the material behavior of the casing can be represented by *effective* properties, we have limited our investigation to wavelengths that are long compared to the representative volume element.

As a result, we can discuss the behavior as $k \rightarrow 0$ but not the asymptotic behavior as $k \rightarrow \infty$. This prevents us from developing a model of the minimum phase velocity of the extensional wave of this system.

Controlling the Maximum Phase Velocity of the Extensional Wave

Since we cannot define a minimum phase velocity of the extensional wave, we cannot define a measure of the dispersion of this mode. However, using equation (38), we can control the maximum phase velocity of the extensional wave.

First, as an example of the effect of the reinforcing fibers on the phase velocity of the extensional wave, we substitute the values of $_1E$, $_1\rho$, $_2E_L$, and $_2\rho$ into equation (38), along with $R = 8.45$, and find that the resulting phase velocity c_B is 1228 m/sec. This value of R resulted in a phase velocity of 1000 m/sec in the composite rod with an isotropic rubber casing. Therefore, the addition of the reinforcing fibers, without changing the value of R, has increased the phase velocity by 23 percent.

Now, by rearranging equation (38) to

$$\sqrt{\frac{\left(_1E - _2E_L - c_B^2 \, _1\rho + c_B^2 \, _2\rho \right)}{\left(c_B^2 \, _2\rho - _2E_L \right)}} \tag{41}$$

and substituting the desired value of $c_B = 1000$ m/sec, we find that R must equal 12.5. This means that, when 10-percent reinforcing fibers are added to the casing, the value of R must increase by 45 percent to maintain a maximum phase velocity of the extensional wave of 1000 m/sec.

The frequency spectrum for the extensional wave in the composite rod with a silica glass core and fiber-reinforced rubber casing is shown in figure 6. This system has an $R = 12.5$ so that the maximum phase velocity is 1000 m/sec. Also shown in figure 6 is the frequency spectrum of the composite rod consisting of the silica glass core and isotropic rubber casing and a line
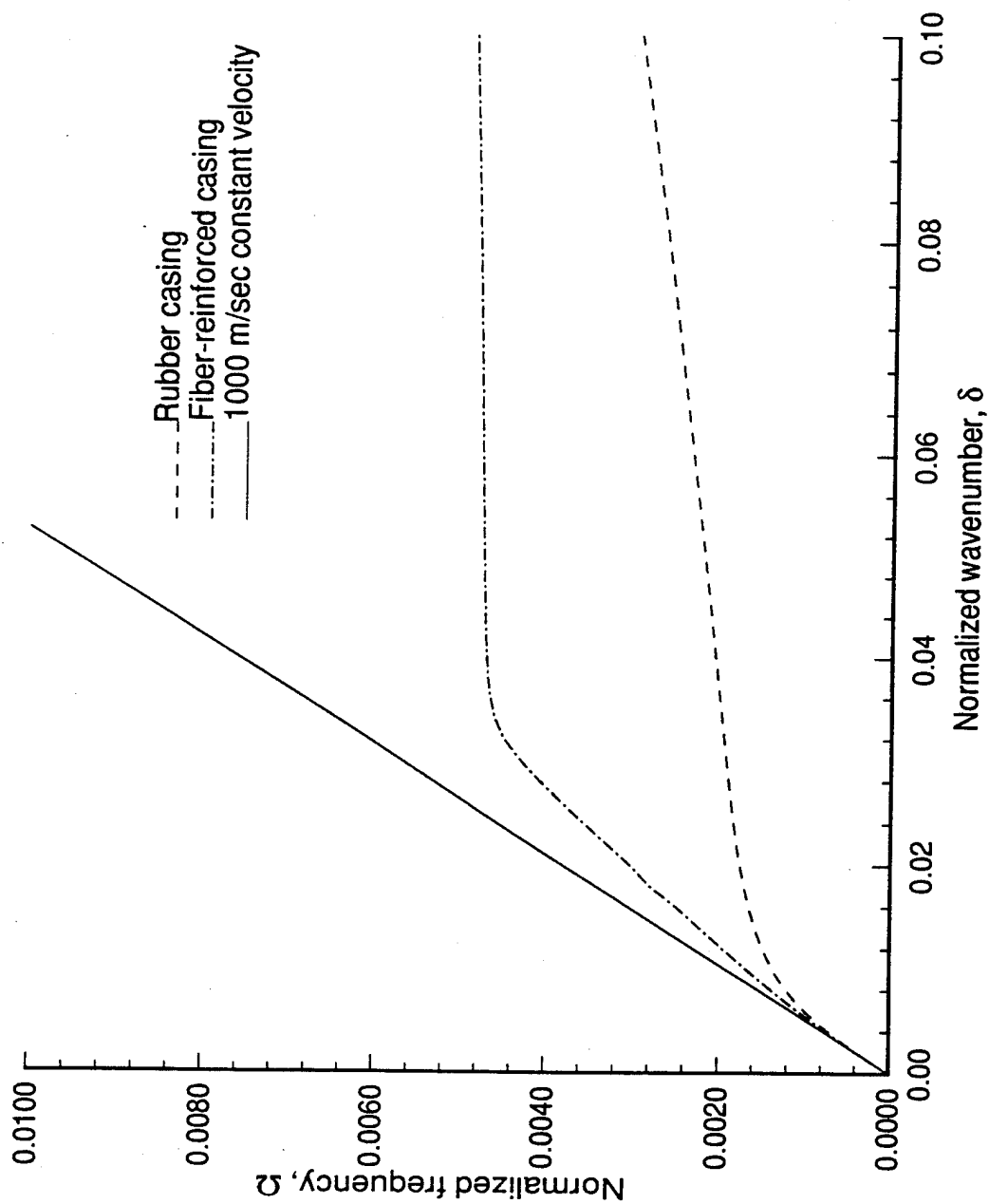
Figure 6. Frequency Spectra of Extensional Waves in Composite Rods With a
Silica Glass Core and a Casing of Isotropic or Fiber-Reinforced Rubber

representing a constant normalized phase velocity of 1000 m/sec. Inspection of figure 6 shows that the extensional wave in the rod with the transversely isotropic casing has a distinct change in phase velocity at approximately $\delta = 0.035$. The model of the extensional wave in the composite rod assumes only axial displacements occur and uses the longitudinal Young's modulus to define the wave velocity. These assumptions are valid in the low wavenumbers, as is evidenced by the agreement with the 1000-m/sec constant phase velocity line. However, as wavenumber increases, radial motions couple into this mode and the simple model is no longer valid.

In the case of the rod with a transversely isotropic casing, $_2E_T \ll {_2}E_L$, and so we might expect that as radial displacements couple into the longitudinal mode, the phase velocity would decrease. In the case of the rod with an isotropic casing, the Young's modulus is constant in all directions. Therefore, we might expect a more gradual change in the phase velocity as the radial displacements begin to couple into this mode. However, these speculations should be validated by an analysis of the mode shapes, which is beyond the scope of this investigation.

Figure 7 shows the same frequency spectra of figure 6 but plotted over a smaller wavenumber and frequency band. This figure emphasizes the nearly linear behavior of the extensional wave at the low wavenumbers and frequencies. The exact phase velocity of the extensional wave at $\delta = 0.01$ in each composite rod is

isotropic casing: $c = 717$ m/sec
transversely isotropic casing: $c = 875$ m/sec.

These results indicate that the rod with the transversely isotropic casing is less dispersive and that at $\delta = 0.01$ the phase velocity of the extensional wave is approximately 12.5 percent less than the maximum phase velocity of 1000 m/sec. The rod with the isotropic rubber casing is the more dispersive, and at $\delta = 0.01$ the phase velocity of the extensional wave is over 28 percent less than the maximum phase velocity.
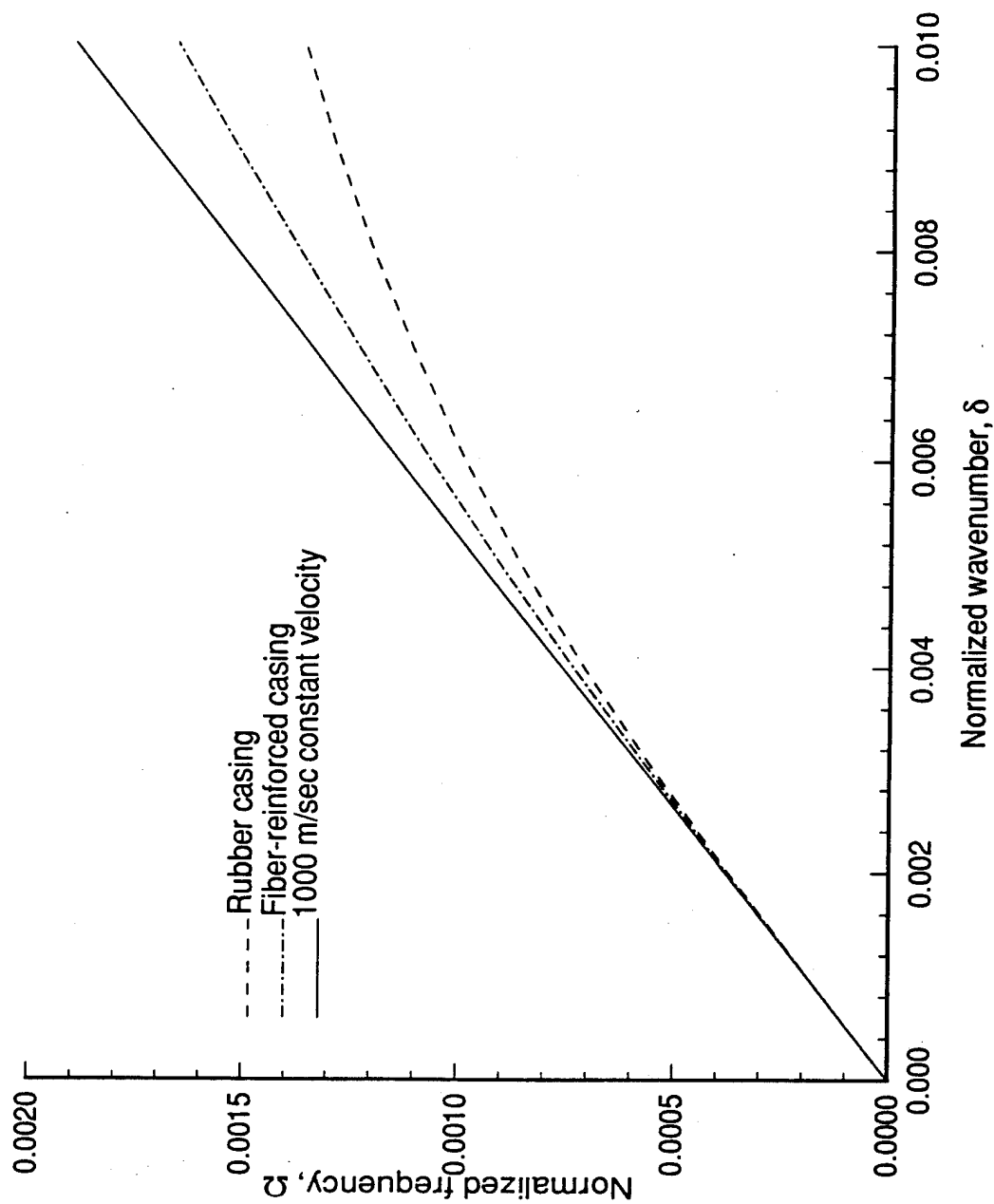
Figure 7. Low Wavenumber-Frequency Spectra of Extensional Waves in Composite Rods With a Silica Glass Core and a Casing of Isotropic or Fiber-Reinforced Rubber

CONCLUSIONS

The maximum phase velocity of the extensional wave in composite rods with isotropic cores and isotropic casings is bounded by the bar wave velocity in the core and the bar wave velocity in the casing. With proper selection of the ratio of the outer radius of the casing and the radius of the core, the maximum phase velocity can be controlled within these bounding velocities. For composite rods composed of isotropic cores and isotropic casings, the extensional wave phase velocity has an asymptotic minimum. This minimum phase velocity can be used to calculate the range of dispersion of the extensional wave. For the types of systems investigated in this report, the minimum phase velocity is the Rayleigh velocity of the casing.

A low-wavenumber model of the maximum phase velocity of extensional waves in composite rods with an isotropic core and a transversely isotropic casing was developed. It was found that when longitudinal reinforcing fibers are added to the casing, the extensional wave phase velocity increases. The maximum phase velocity of this system is also bounded by the bar wave velocity in the core and the bar wave velocity in the casing, where the bar wave velocity of the casing is defined by the effective longitudinal Young's modulus and the effective density of the transversely isotropic material.

REFERENCES

Achenbach, J. D. (1987), *Wave Propagation in Elastic Solids*, Fifth printing, Elseivier Science Publishing Company, Inc., New York, NY.

Armenakas, A. E. (1965), "Torsional Waves in Composite Rods," *Journal of the Acoustical Society of America* **38**, 439-446

Berliner, M. J. (1995), "Wave Propagation in a Fluid-Loaded, Homogeneous, Transversely Isotropic, Elastic Cylinder of Arbitrary Thickness," NUWC-NPT Technical Report 10,845, Naval Undersea Warfare Center Detachment, New London, CT.

Chree, C. (1889), "The Equations of an Isotropic Elastic Solid in Polar and Cylindrical Coordinates, Their Solutions and Applications," *Quarterly Journal of Pure and Applied Mathematics* **14**, 250-369.

Chree, C. (1890), "On the Longitudinal Vibrations of Aeolotropic Bars With One Axis of Material Symmetry," *Quarterly Journal of Mathematics* **24**, 340-354.

Christensen, R. M. (1979), *Mechanics of Composite Materials*, John Wiley & Sons, New York.

Fung, Y. C. (1977), *A First Course in Continuum Mechanics*, Second printing, Prentice-Hall, Inc., Englewood Cliffs, New Jersey.

Hashin, Z. (1979), "Analysis of Properties of Fiber Composites 'With Anisotropic Constituents," *Journal of Applied Mechanics* **46**, 543-550.

Hashin, Z. (1983), "Analysis of Composite Materials - A Survey," *Journal of Applied Mechanics* **50**, 481-505.

Jones, R. M. (1975), *Mechanics of Composite Materials*, Scripta Book Company, Washington, D.C.

Lai, J. (1971), "Propagation of Harmonic Waves in a Composite Elastic Cylinder," *Journal of the Acoustical Society of America* **49**, 220-228.

McNiven, H. D., and Y. Mengi (1967), "Controlled Dispersion of Axisymmetric Waves in Composite Rods," *Journal of the Acoustical Society of America* **43**, 691-696.

McNiven, H. D., J. L. Sackman, and A. H. Shah (1963), "Dispersion of Axially Symmetric Waves in Composite, Elastic Rods," *Journal of the Acoustical Society of America* **35**, 1602-1609.

Mengi, Y., and H. D. McNiven (1967), "Asymptotic Phase Velocities of Axisymmetric Waves in Composite Rods," *Journal of the Acoustical Society of America* **42**, 66-72.

Mirsky, I. (1965a), "Wave Propagation in Transversely Isotropic Circular Cylinders, Part I: Theory," *Journal of the Acoustical Society of America* **37**, 1016-1021.

Mirsky, I. (1965b), "Wave Propagation in Transversely Isotropic Circular Cylinders, Part II: Numerical Results," *Journal of the Acoustical Society of America* **37**, 1022-1026.

Morse, R. W. (1954), "Compressional Waves Along an Anisotropic Circular Cylinder Having Hexagonal Symmetry," *Journal of the Acoustical Society of America* **26**, 1018-1021.

Pochhammer, L. (1876), "Uber die Fortpflanzungsgeschwindigkeiten kleiner Schwingungen in einem unbegrenzten isotropen Kreiscyclinder," *Journal fur Mathematik* (Crelle) **81**, 324-336.

Press, W. H., B. P. Flannery, S. A. Teukolsky, and W. T. Vettering (1986), *Numerical Recipes: The Art of Scientific Computing*, Cambridge University Press, New York, NY.

Sokolnikoff, I. S. (1987), *Mathematical Theory of Elasticity*, Reprint Edition, Krieger Publishing Company, Malabar, FL.

APPENDIX A. BOUNDARY EQUATIONS

$$L_{1,1} = -2\frac{{}_1c_{66}}{a}A_{11}\,J_n({}_1\zeta_1 a)_{,a} + 2{}_1c_{66}\frac{n^2}{a^2}A_{11}\,J_n({}_1\zeta_1 a)$$

$$+\left(i\,{}_1c_{13}\,{}_1\eta_1 k - {}_1c_{11}\,{}_1\zeta_1^2\right)A_{11}\,J_n({}_1\zeta_1 a) \tag{A-1}$$

$$L_{1,2} = -2\frac{{}_1c_{66}}{a}A_{21}\,J_n({}_1\zeta_2 a)_{,a} + 2{}_1c_{66}\frac{n^2}{a^2}A_{21}\,J_n({}_1\zeta_2 a)$$

$$+\left(i\,{}_1c_{13\,.1}\eta_2 k - {}_1c_{11}\,{}_1\zeta_2^2\right)A_{21}\,J_n({}_1\zeta_2 a) \tag{A-2}$$

$$L_{1,3} = 2{}_1c_{66}\frac{n}{a}\left(A_{31}\,J_n({}_1\zeta_3 a)_{,a} - \frac{1}{a}A_{31}\,J_n({}_1\zeta_3 r)\right) \tag{A-3}$$

$$L_{1,4} = 2\frac{{}_2c_{66}}{a}A_{12}\,J_n({}_2\zeta_1 a)_{,a} - 2{}_2c_{66}\frac{n^2}{a^2}A_{12}\,J_n({}_2\zeta_1 a)$$

$$-\left(i\,{}_2c_{13}\,{}_2\eta_1 k - {}_2c_{11}\,{}_2\zeta_1^2\right)A_{12}\,J_n({}_2\zeta_1 a) \tag{A-4}$$

$$L_{1,5} = 2\frac{{}_2c_{66}}{a}B_{12}\,Y_n({}_2\zeta_1 a)_{,a} - 2{}_2c_{66}\frac{n^2}{a^2}B_{12}\,Y_n({}_2\zeta_1 a)$$

$$-\left(i\,{}_2c_{13}\,{}_2\eta_1 k - {}_2c_{11}\,{}_2\zeta_1^2\right)B_{12}\,Y_n({}_2\zeta_1 a) \tag{A-5}$$

$$L_{1,6} = 2\frac{{}_2c_{66}}{a}A_{22}\,J_n({}_2\zeta_2 a)_{,a} - 2{}_2c_{66}\frac{n^2}{a^2}A_{22}\,J_n({}_2\zeta_2 a)$$

$$-\left(i\,{}_2c_{13}\,{}_2\eta_2 k - {}_2c_{11}\,{}_2\zeta_2^2\right)A_{22}\,J_n({}_2\zeta_2 a) \tag{A-6}$$

$$L_{1,7} = 2\frac{{}_2c_{66}}{a}B_{22}\,Y_n({}_2\zeta_2 a)_{,a} - 2{}_2c_{66}\frac{n^2}{a^2}B_{22}\,Y_n({}_2\zeta_2 a)$$

$$-\left(i\,{}_2c_{13}\,{}_2\eta_2 k - {}_2c_{11}\,{}_2\zeta_2^2\right)B_{22}\,Y_n({}_2\zeta_2 a) \tag{A-7}$$

$$L_{1,8} = -2{}_2c_{66}\frac{n}{a}\left(A_{32}\,J_n({}_2\zeta_3 a)_{,a} + \frac{1}{a}A_{32}\,J_n({}_2\zeta_3 a)\right) \tag{A-8}$$

$$L_{1,9} = -2{}_2c_{66}\frac{n}{a}\left(B_{32}\,Y_n({}_2\zeta_3 a)_{,a} + \frac{1}{a}B_{32}\,Y_n({}_2\zeta_3 a)\right) \tag{A-9}$$

$$L_{2,1} = {}_1c_{44}\left({}_1\eta_1 + ik\right)A_{11}\,J_n({}_1\zeta_1 a)_{,a} \tag{A-10}$$

$$L_{2,2} = (_1\eta_2 + ik) A_{21} J_n (_1\zeta_2 a)_{,a} \tag{A-11}$$

$$L_{2,3} = ik\frac{n}{a}A_{31} J_n (_1\zeta_3 a) \tag{A-12}$$

$$L_{2,4} = -_2c_{44} (_2\eta_1 + ik) A_{12} J_n (_2\zeta_1 a)_{,a} \tag{A-13}$$

$$L_{2,5} = -_2c_{44} (_2\eta_1 + ik) B_{12} Y_n (_2\zeta_1 a)_{,a} \tag{A-14}$$

$$L_{2,6} = - (_2\eta_2 + ik) A_{22} J_n (_2\zeta_2 a)_{,a} \tag{A-15}$$

$$L_{2,7} = - (_2\eta_2 + ik) B_{22} Y_n (_2\zeta_2 a)_{,a} \tag{A-16}$$

$$L_{2,8} = -ik\frac{n}{a}A_{32} J_n (_2\zeta_3 a) \tag{A-17}$$

$$L_{2,9} = -ik\frac{n}{a}B_{32} Y_n (_2\zeta_3 a) \tag{A-18}$$

$$L_{3,1} = _1c_{66}\left(2\frac{n}{a^2}A_{11} J_n (_1\zeta_1 a) -2\frac{n}{a}A_{11} J_n (_1\zeta_1 a)_{,a} \right) \tag{A-19}$$

$$L_{3,2} = _1c_{66}\left(2\frac{n}{a^2}A_{21} J_n (_1\zeta_2 a) -2\frac{n}{a}A_{21} J_n (_1\zeta_2 a)_{,a} \right) \tag{A-20}$$

$$L_{3,3} = _1\zeta_3^2 A_{31} J_n (_1\zeta_3 a) + \frac{2}{a}A_{31} J_n (_1\zeta_3 a)_{,a} - 2\frac{n^2}{a^2}A_{31} J_n (_1\zeta_3 r) \tag{A-21}$$

$$L_{3,4} = -_2c_{66}\left(2\frac{n}{a^2}A_{12} J_n (_2\zeta_1 a) -2\frac{n}{a}A_{12} J_n (_2\zeta_1 a)_{,a} \right) \tag{A-22}$$

$$L_{3,5} = -_2c_{66}\left(2\frac{n}{a^2}B_{12} Y_n (_2\zeta_1 a) -2\frac{n}{a}B_{12} Y_n (_2\zeta_1 a)_{,a} \right) \tag{A-23}$$

$$L_{3,6} = -_2c_{66}\left(2\frac{n}{a^2}A_{22} J_n (_2\zeta_2 a) -2\frac{n}{a}A_{22} J_n (_2\zeta_2 a)_{,a} \right) \tag{A-24}$$

A-2

$$L_{3,7} = -2c_{66}\left(2\frac{n}{a^2}B_{22}\,Y_n\,(_2\zeta_2a) - 2\frac{n}{a}B_{22}\,Y_n\,(_2\zeta_2a)_{,a}\right)$$

(A-25)

$$L_{3,8} = -2\zeta_3^2 A_{32}\,J_n\,(_2\zeta_3a) + \frac{2}{a}A_{32}\,J_n\,(_2\zeta_3a)_{,a} - 2\frac{n^2}{a^2}A_{32}\,J_n\,(_2\zeta_3a)$$

(A-26)

$$L_{3,9} = -2\zeta_3^2 B_{32}\,Y_n\,(_2\zeta_3a) + \frac{2}{a}B_{32}\,Y_n\,(_2\zeta_3a)_{,a} - 2\frac{n^2}{a^2}B_{32}\,Y_n\,(_2\zeta_3a)$$

(A-27)

$$L_{4,1} = A_{11}\,J_n\,(_1\zeta_1a)_{,a}$$

(A-28)

$$L_{4,2} = A_{21}\,J_n\,(_1\zeta_2a)_{,a}$$

(A-29)

$$L_{4,3} = \frac{n}{a}A_{31}\,J_n\,(_1\zeta_3a)$$

(A-30)

$$L_{4,4} = -A_{12}\,J_n\,(_2\zeta_1a)_{,a}$$

(A-31)

$$L_{4,5} = -B_{12}\,Y_n\,(_2\zeta_1a)_{,a}$$

(A-32)

$$L_{4,6} = -A_{22}\,J_n\,(_2\zeta_2a)_{,a}$$

(A-33)

$$L_{4,7} = -B_{22}\,Y_n\,(_2\zeta_2a)_{,a}$$

(A-34)

$$L_{4,8} = -\frac{n}{a}A_{32}\,J_n\,(_2\zeta_3a)$$

(A-35)

$$L_{4,9} = -\frac{n}{a}B_{32}\,Y_n\,(_2\zeta_3a)$$

(A-36)

$$L_{5,1} = -\frac{n}{a}A_{11}\,J_n\,(_1\zeta_1a)$$

(A-37)

$$L_{5,2} = -\frac{n}{a}A_{21}\,J_n\,(_1\zeta_2a)$$

(A-38)

$$L_{5,3} = -A_{31}\,J_n\,(_1\zeta_3a)_{,a}$$

(A-39)

$$L_{5,4} = \frac{n}{a} A_{12} \, J_n \left({}_2\zeta_1 a \right) \tag{A-40}$$

$$L_{5,5} = \frac{n}{a} B_{12} \, Y_n \left({}_2\zeta_1 a \right) \tag{A-41}$$

$$L_{5,6} = \frac{n}{a} A_{22} \, J_n \left({}_2\zeta_2 a \right) \tag{A-42}$$

$$L_{5,7} = \frac{n}{a} B_{22} \, Y_n \left({}_2\zeta_2 a \right) \tag{A-43}$$

$$L_{5,8} = A_{32} \, J_n \left({}_2\zeta_3 a \right)_{,a} \tag{A-44}$$

$$L_{5,9} = B_{32} \, Y_n \left({}_2\zeta_3 a \right)_{,a} \tag{A-45}$$

$$L_{6,1} = {}_1\eta_1 A_{11} \, J_n \left({}_1\zeta_1 a \right) \tag{A-46}$$

$$L_{6,2} = {}_1\eta_2 A_{21} \, J_n \left({}_1\zeta_2 a \right) \tag{A-47}$$

$$L_{6,3} = 0 \tag{A-48}$$

$$L_{6,4} = -{}_2\eta_1 A_{12} \, J_n \left({}_2\zeta_1 a \right) \tag{A-49}$$

$$L_{6,5} = -{}_2\eta_1 B_{12} \, Y_n \left({}_2\zeta_1 a \right) \tag{A-50}$$

$$L_{6,6} = -{}_2\eta_2 A_{22} \, J_n \left({}_2\zeta_2 a \right) \tag{A-51}$$

$$L_{6,7} = -{}_2\eta_2 B_{22} \, Y_n \left({}_2\zeta_2 a \right) \tag{A-52}$$

$$L_{6,8} = 0 \tag{A-53}$$

$$L_{6,9} = 0 \tag{A-54}$$

$$L_{7,1} = 0 \tag{A-55}$$

$$L_{7,2} = 0 \tag{A-56}$$

$$L_{7,3} = 0 \tag{A-57}$$

$$L_{7,4} = 2\frac{2^{c_{66}}}{b}A_{12}\,J_n\left(2\zeta_1 b\right)_{,b} - 2\,2^{c_{66}}\frac{n^2}{b^2}A_{12}\,J_n\left(2\zeta_1 b\right)$$
$$-\left(i\,2^{c_{13}}\,2\eta_1 k - 2^{c_{11}}\,2\zeta_1^2\right)A_{12}\,J_n\left(2\zeta_1 b\right) \tag{A-58}$$

$$L_{7,5} = 2\frac{2^{c_{66}}}{b}B_{12}\,Y_n\left(2\zeta_1 b\right)_{,b} - 2\,2^{c_{66}}\frac{n^2}{b^2}B_{12}\,Y_n\left(2\zeta_1 b\right)$$
$$-\left(i\,2^{c_{13}}\,2\eta_1 k - 2^{c_{11}}\,2\zeta_1^2\right)B_{12}\,Y_n\left(2\zeta_1 b\right) \tag{A-59}$$

$$L_{7,6} = 2\frac{2^{c_{66}}}{b}A_{22}\,J_n\left(2\zeta_2 b\right)_{,b} - 2\,2^{c_{66}}\frac{n^2}{b^2}A_{22}\,J_n\left(2\zeta_2 b\right)$$
$$-\left(i\,2^{c_{13}}\,2\eta_2 k - 2^{c_{11}}\,2\zeta_2^2\right)A_{22}\,J_n\left(2\zeta_2 b\right) \tag{A-60}$$

$$L_{7,7} = 2\frac{2^{c_{66}}}{b}B_{22}\,Y_n\left(2\zeta_2 b\right)_{,b} - 2\,2^{c_{66}}\frac{n^2}{b^2}B_{22}\,Y_n\left(2\zeta_2 b\right)$$
$$-\left(i\,2^{c_{13}}\,2\eta_2 k - 2^{c_{11}}\,2\zeta_2^2\right)B_{22}\,Y_n\left(2\zeta_2 b\right) \tag{A-61}$$

$$L_{7,8} = -2\,2^{c_{66}}\frac{n}{b}\left(A_{32}\,J_n\left(2\zeta_3 b\right)_{,b} + \frac{1}{b}A_{32}\,J_n\left(2\zeta_3 b\right)\right) \tag{A-62}$$

$$L_{7,9} = -2\,2^{c_{66}}\frac{n}{b}\left(B_{32}\,Y_n\left(2\zeta_3 b\right)_{,b} + \frac{1}{b}B_{32}\,J_n\left(2\zeta_3 b\right)\right) \tag{A-63}$$

$$L_{8,1} = 0 \tag{A-64}$$

$$L_{8,2} = 0 \tag{A-65}$$

$$L_{8,3} = 0 \tag{A-66}$$

$$L_{8,4} = -2^{c_{44}}\left(2\eta_1 + ik\right)A_{12}\,J_n\left(2\zeta_1 b\right)_{,b} \tag{A-67}$$

$$L_{8,5} = -2^{c_{44}}\left(2\eta_1 + ik\right)B_{12}\,Y_n\left(2\zeta_1 b\right)_{,b} \tag{A-68}$$

$$L_{8,6} = -(_2\eta_2 + ik) A_{22} J_n (_2\zeta_2 b)_{,b}$$

$$(A-69)$$

$$L_{8,7} = -(_2\eta_2 + ik) B_{22} Y_n (_2\zeta_2 b)_{,b}$$

$$(A-70)$$

$$L_{8,8} = -ik\frac{n}{b}A_{32} J_n (_2\zeta_3 b)$$

$$(A-71)$$

$$L_{8,9} = -ik\frac{n}{b}B_{32} Y_n (_2\zeta_3 b)$$

$$(A-72)$$

$$L_{9,1} = 0$$

$$(A-73)$$

$$L_{9,2} = 0$$

$$(A-74)$$

$$L_{9,3} = 0$$

$$(A-75)$$

$$L_{9,4} = -_2c_{66}\left(2\frac{n}{b^2}A_{12} J_n (_2\zeta_1 b) - 2\frac{n}{b}A_{12} J_n (_2\zeta_1 b)_{,b} \right)$$

$$(A-76)$$

$$L_{9,5} = -_2c_{66}\left(2\frac{n}{b^2}B_{12} Y_n (_2\zeta_1 b) - 2\frac{n}{b}B_{12} Y_n (_2\zeta_1 b)_{,b} \right)$$

$$(A-77)$$

$$L_{9,6} = -_2c_{66}\left(2\frac{n}{b^2}A_{22} J_n (_2\zeta_2 b) - 2\frac{n}{b}A_{22} J_n (_2\zeta_2 b)_{,b} \right)$$

$$(A-78)$$

$$L_{9,7} = -_2c_{66}\left(2\frac{n}{b^2}B_{22} Y_n (_2\zeta_2 b) - 2\frac{n}{b}B_{22} Y_n (_2\zeta_2 b)_{,b} \right)$$

$$(A-79)$$

$$L_{9,8} = -_2\zeta_3^2 A_{32} J_n (_2\zeta_3 b) + \frac{2}{b}A_{32} J_n (_2\zeta_3 b)_{,b} - 2\frac{n^2}{b^2}A_{32} J_n (_2\zeta_3 b)$$

$$(A-80)$$

$$L_{9,9} = -_2\zeta_3^2 B_{32} Y_n (_2\zeta_3 b) + \frac{2}{b}B_{32} Y_n (_2\zeta_3 b)_{,b} - 2\frac{n^2}{b^2}B_{32} Y_n (_2\zeta_3 b)$$

$$(A-81)$$

INITIAL DISTRIBUTION LIST

Addressee	No. of Copies
Defense Technical Information Center	12
Office of Naval Research (Code 321SS: K. Dial, S. Littlefield, R. Varley)	3
Naval Research Laboratory (A. Dandridge, S. Vohra)	2
Cambridge Acoustical Associates (J. Garrelick, J. Cole III)	2
Applied Measurement Systems, Inc., New London (J. Diggs)	1